

مخطط للعلامة المائبة المعتمدة على تكيف صورة DCT-SVD بخصائص الانسان المرئية

*جاستين فارجسي، *سعودية سوباش، *عمر بن حسين، ***محمد رمضان سعدي،

***بيجوي بابو و ***محمد رياض الدين

*كلية علوم الحاسب - جامعه الملك خالد- ابها - المملكة العربية السعودية

**مركز تقنية وهندسة المعلومات - جامعة مانو غنانيا مسندرانار - الهند

***كلية العلوم- جامعه جنوب الوادي - قنا - مصر

الخلاصة

هذا البحث يقدم مخطط مقترح لكفاءة العلامة المائبة بدمج كلاً من تقسيم القيمة الأحادية (SVD) مع محول جيب التمام المتقطع (DCT) مع المعلومات المتجانسة للصورة الناقله. الخوارزمية المقترحة تقوم بتقسيم الصورة الناقله وصورة العلامة المائبة الى كتل غير متداخلة ثم تحليل البكسلات المتجانسة لهما للتعرف على أفضل الكتل المحتملة للصورة الناقله مع كتله العلامة المائبة المناسبة التي يتم الحاقها بحيث أن تحافظ العلامة المائبة على أفضل صورة مرئية، والخوارزمية التي تتجنب تقسيم التردد العالي لكتل الصورة الناقله لدمج كتل العلامة المائبة تجعل الصورة البصرية ذات علامة مائبة غير مشوهه. النتائج التجريبية أظهرت أن الخوارزمية المقترحة تنتج نوعية جيدة للعلامة المائبة للصور وتكون محصنة ضد أي هجمات محتمله.

Image adaptive DCT- SVD based digital watermarking scheme by human visual characteristics

Justin Varghese*, Saudia Subash**, Omer Bin Hussain*, Mohammed Ramadan Saady***, Bijoy Babu*** and Mohammed Riazuddin***

**College of Computer Science, King Khalid University, Abha, Saudi Arabia*

E-mail: justin_var@yahoo.com

***Centre for Information Technology & Engineering, Manonmaniam Sundaranar University, India.*

**** College of Science, South Valley University, Egypt.*

ABSTRACT

The paper proposes an efficient watermarking scheme by incorporating singular value decomposition (SVD), discrete cosine transform (DCT) and homogeneity information in the carrier image. The algorithm decomposes the carrier and watermark images into non-overlapping blocks and analyzes the homogeneity of pixels in them to identify the possible blocks of carrier image where the suitable watermark block can be attached so that the watermarking process maintain better visual image fidelity in the watermarked image. The algorithm avoids the decomposed high frequency carrier image blocks while attaching watermark blocks to reduce the visual distortion in the watermarked images. Experimental results show that the proposed algorithm produces good quality watermarked images and are less immune to potential attacks.

Keywords: Copyright protection; discrete wavelet transform (DWT); image watermarking; singular value decomposition (SVD)

INTRODUCTION

The advancement of information technology made the access of digital documents, audio, images, text and video simple through internet. This made numerous digital flaws in information protection like illegal copying, forgery, copy-right protection and ownership identity of digital data and hence the digital watermarking techniques for ownership-rights preservation of digital documents became significant for all domains involved in digital transmission (Ingemar *et al.*, 2008). These watermarking techniques are broadly classified in to spatial and frequency domain techniques of which the frequency domain techniques ranked high due to its signal spreading capability and that the watermarked images produced by the transform based algorithm are not

much sensitive to potential attacks (Juergen, 2005). In frequency domain methods, the embedding of watermark image in carrier image takes place in the transformed coefficients of frequency domain transformations like discrete cosine transform (DCT), discrete wavelet transform (DWT), singular value decomposition (SVD) etc. (Juergen, 2005). Haar DWT decomposes the image in to four frequency bands, low low (LL), low high (LH) and high high (HH) and these frequency bands respectively contains approximation, horizontal, vertical and diagonal details of the image (Gonzalez *et al.*, 2008). Among these transform based watermarking algorithms; the SVD based algorithms produce better results due to its simplicity and robustness (Hailiang *et al.*, 2012; Wang *et al.*, 2011). The algorithm proposed by incorporating DCT and SVD transforms (Alexander *et al.*, 2006) showed much deviation from the original carrier image and the watermarked images are very much sensitive to external attacks. The watermarking algorithm proposed by incorporating DWT and SVD transforms (Emir *et al.*, 2004) though is less sensitive to potential attacks, failed to maintain good quality in the watermarked images since it attaches watermark to all the frequency components of DWT. The two algorithms (Ray-Shine *et al.*, 2012) proposed by respectively addressing the limitations of other algorithms (Alexander *et al.*, 2006; Emir *et al.*, 2004) attached principal component of the watermark to the singular values of the transformed carrier image. But the algorithms are very sensitive to potential attacks. Chih-Chin (2010) proposed an algorithm by addressing the limitations of Emir *et al.* (2004) algorithm and it attached the copies of watermark to only high low (HL) and low high (LH) frequencies of Haar DWT but the algorithm produced distortion in the watermarked images due to the lack of homogeneity analysis among pixels of the carrier image. The algorithm proposed by Jen-Sheng *et al.*, (2011) incorporated feature set selection and attack resistant schemes in extraction process, but is computationally inefficient due to the various optimization iterations by the genetic algorithm. Hailiang *et al.*, (2012) proposed a rotation, scaling and translation (RST) invariant watermarking algorithm by incorporating DWT and SVD, the algorithm attached the encrypted watermark images to the approximation sub band of DWT but failed to address other potential attacks. Further, the algorithm is not capable of producing good quality watermarked images since it consumes much of the low frequency components of carrier image by embedding watermarks in approximation component of the carrier image. The algorithm proposed by Mitra *et al.*, (2012) used SVD and QR transformations to attach watermark in the lowest frequencies of contourlet transform, but the algorithm produced distinguishable distortions in the extracted watermarked images in case where the carrier image undergoes external potential attacks. QR transformation is a matrix decomposition technique, where any matrix, A can be written as $A=QR$ such that Q is an orthogonal matrix and R is an upper triangular matrix. The image adaptive watermarking algorithm proposed by Paul B. *et al.*, (2005) incorporated wavelet and SVD transformations in the watermarking scheme but the algorithm is very sensitive

to potential attacks. Also, the algorithm attaches only binary watermark images and it became computationally inefficient, since it used vector quantization algorithm for the optimization of adaptive quantization parameters, while indexing the blocks. Many other algorithms (Bhosale *et al.*, 2012; Chen *et al.*, 2012; Coatrieux *et al.*, 2012; Ishikawa *et al.*, 2012; Kandpal *et al.*, 2012; Vargas *et al.*, 2013; Varghese *et al.*, 2014; Walia *et al.*, 2013; Wang *et al.*, 2011; Wang *et al.*, 2012; Wu *et al.*, 2005; Yang *et al.*, 2010; Zareian *et al.*, 2013) also developed in the literature by meeting some requirements of watermarking, but these algorithms also failed in simultaneously meeting other vital requirements of watermarking (Mason *et al.*, 2000) including perceptibility, robustness, orthogonality, protection against attacks etc.

Among all transform based watermarking techniques, DCT has the advantage of computational efficiency in providing frequency bands and also has high resistance to the potential attacks like compression, filtering and noise (Koch *et al.*, 1996). The singular values of SVD is a diagonal matrix that have good stability to the added perturbation, when an image is affected with potential attacks and it also have resistance towards transpose, flip, rotation, scaling and translation based attacks (Jie *et al.*, 2006; Zhou *et al.*, 2004). In this paper, we propose an image adaptive SVD - DCT based algorithm for digital watermarking by analyzing the homogeneity among pixels of carrier and watermark images. Unlike other DCT- SVD based algorithms (Alexander *et al.*, 2006; Ray-Shine *et al.*, 2012), that attach watermark components to all the frequency components, the proposed algorithm attach the watermark components to the frequency components of selected visually non-sensitive blocks of the carrier images in order to provide high visual quality in the watermarked image.

THE PROPOSED ALGORITHM

The homogeneity information among pixels in the blocks of the carrier and watermark images are analyzed by the proposed algorithm so that the embedding process does not produce severe visual distortions in the watermarked image. The high frequency blocks of watermark image are attached to the high frequency blocks of the carrier image. Moreover, the algorithm avoids the carrier image blocks with sharp edges from attaching watermark blocks in order to maintain visual fidelity in the watermarked image. The sharp edges are determined by Sobel edge detection algorithm (Gonzalez *et al.*, 2008) due to its simplicity and effectiveness in detecting sharp edges of all directions. The proposed algorithm includes two distinct stages of embedding and extraction of the watermark from the carrier image. The embedding and extraction stages are explained in the following subsections.

The embedding algorithm

The embedding algorithm first makes use of Sobel edge detection algorithm (Gonzalez *et al.*, 2008) to avoid the carrier image areas with sharp edges and then finds the

remaining high frequency non-overlapping blocks of carrier image to attach the non-overlapping blocks of watermark image. The algorithm attaches high frequency blocks of carrier image to the high frequency blocks of watermark image in the DCT- SVD domain to maintain image quality in the watermarked images. If A and W denote the carrier and watermark images respectively of sizes $M_1 \times N_1$, $M_2 \times N_2$, the embedding algorithm can be tracked through following 9 steps.

Step 1: The algorithm first performs edge detection using Sobel method on the carrier image to find edge image, E . The sharp edge areas of carrier image are determined in the binary image, ET by applying a high threshold, T to the edge image, E as

$$ET_i = \begin{cases} 1 & \text{if } E_i \geq T \\ 0 & \text{Otherwise} \end{cases}, \forall i = (x_1, x_2) \in \text{domain}(E) \quad (1)$$

The $\text{domain}(E)$ denotes all the pixel positions of the edge image, E .

Step 2: The input carrier image A is decomposed in to N non overlapping blocks Bl starting at each (i_l, j_l) of size $(n_l \times n_l)$ such that,

$$Bl_i = \{ A_{k,l} : i_l \leq k < i_l + n_l, j_l \leq l < j_l + n_l \} \quad (2)$$

and

$$Ed_i = \sum_{x_l=i_l}^{i_l+n_l-1} \sum_{y_l=j_l}^{j_l+n_l-1} ET_{x_l, y_l} \quad (3)$$

where

$$\bigcup_{l=0}^{N-1} Bl_i = A \quad (4)$$

and

$$(i_l, j_l) \in \left\{ (c_1 \cdot n_l, c_2 \cdot n_l) : 0 \leq c_1 < \frac{M_l}{4}, 0 \leq c_2 < \frac{N_l}{4} \right\} \quad (5)$$

Note that (i_l, j_l) denotes the starting position of each non overlapping block and Ed_i shows the presence of edges in block i . From among all blocks of carrier image, the algorithm avoids all blocks of carrier image that having sharp edges as $Ed_i \neq 0$ to reduce the distortions in watermarked images.

Step 3: The algorithm analyzes the homogeneity of pixels in the block by finding the standard deviation, σ^2 corresponding to all blocks Bl_i where $Ed_i = 0$ as

$$\sigma^2 (Bl_i) = \sqrt{\frac{1}{(n_l \times n_l)} \sum_{i=1}^{n_l \times n_l} (x_i - \mu)^2} \quad (6)$$

where $x = [x_1, x_2, \dots, x_{n_1 \times n_1}] \in Bl_i$, μ is the mean of x and $i=0, 1, 2, \dots, N-1$.

Step 4: The carrier image blocks are sorted by standard deviation in descending order as $SBl = [Bl_{k_1}, Bl_{k_2}, \dots, Bl_{k_N}]$

$$\text{such that } \sigma^2(Bl_{k_1}) \geq \sigma^2(Bl_{k_2}) \geq \dots \sigma^2(Bl_{k_N})$$

Here k_1, k_2, \dots, k_n are the block indices.

Step 5: The watermark image W is decomposed in to non overlapping blocks WBl_l starting at each (i_2, j_2) to analyze the homogeneity of watermark blocks as in (2) of size $(n_1 \times n_1)$ such that

$$WBl_i = \{W_{k,l} : i_2 \leq k < i_2 + n_1, j_2 \leq l < j_2 + n_1\} \tag{7}$$

where

$$\bigcup_{l=0}^{M-1} WBl_i = W \tag{8}$$

and

$$(i_1, j_1) \in \left\{ (c_1 \cdot n_1, c_2 \cdot n_1) : 0 \leq c_1 < \frac{M_2}{4}, 0 \leq c_2 < \frac{N_2}{4} \right\} \tag{9}$$

Here (i_1, j_1) denotes the starting position of each non overlapping watermark block.

Step 6: The standard deviation $\sigma^2(WBl_l)$ for all $l=0, 1, 2, \dots, M-1$ in each of the individual blocks WBl_l is found as in (6)

Step 7: Accordingly as in step: 3, the carrier image blocks are sorted by standard deviation as

$$SWBl = [SWBl_{l_1}, SWBl_{l_2}, \dots, SWBl_{l_N}] \tag{10}$$

such that

$$\sigma^2(WBl_{l_1}) \geq \sigma^2(WBl_{l_2}) \geq \dots \sigma^2(WBl_{l_m}) \tag{11}$$

Step 8: For each $SBl_i \in SBl$ and $SWBl_l \in SWBl$ the following sub-steps are performed by

Step 8.1: Apply DCT transform respectively to both SBl_i and $SWBl_l$ to get the DCT applied blocks $DSWBl_i$ and $DSBl_i$

Step 8.2: Apply SVD respectively to both SBl_i and $SWBl_l$ as

$$DSWBl_i = U_i^w \sum_i^w V_i^w \tag{12}$$

and

$$DSBl_i = U_i \sum_i V_i' \quad (13)$$

Step 8.3: Once the DCT of carrier and watermark blocks are determined, the algorithm attaches the singular value component of the watermark block, \sum^w to the respective singular value component \sum of the first M blocks of the carrier image, A which has the maximum standard deviation as

$$\sum_i^* = \sum_i + \alpha \cdot \sum_i^w \quad \forall 0 \leq l < M \quad (14)$$

and

$$\sum_i^* = \sum_i \quad \forall M \leq i < N \quad (15)$$

Here α is scaling parameter used for controlling the strength of watermark embedding. This step embeds the watermark singular values to the corresponding carrier blocks.

Step 8.4: After embedding all blocks of watermark image to the respective blocks of carrier image, the blocks, B_l of the watermarked image are reconstructed by performing the inverses of SVD and DCT as

$$\tilde{B}_l = \begin{cases} IDCT(U_i \sum_i^* V_i') & \text{if } 0 \leq i \leq M \\ B_l & \text{Otherwise} \end{cases} \quad (16)$$

Here $IDCT$ represents inverse DCT.

Step 9: Once the embedding process is over, the embedding scheme reconstructs the watermarked image A by remapping the individual B_l to the respective position by performing the inverse of Step 2.

The proposed algorithm attaches the high frequency watermark blocks to the high frequency blocks of the carrier image by avoiding the blocks of carrier image with sharp edges. For performing the same, the algorithm analyzed the individual watermark and carrier blocks with standard deviation. The embedding process of the proposed algorithm is done in the DCT- SVD domain using Equation (14). Finally the inverses of SVD and DCT are taken to produce the final watermark image. The block diagram of the proposed scheme is shown in Figure1. Unlike other algorithms (Alexander *et al.*, 2006; Ray-Shine *et al.*, 2012) in DCT- SVD domain for digital watermarking, since the proposed algorithm selected less sensitive blocks for human perception by determining standard deviation to attach the watermark components, it always maintains better visual quality in the watermarked images, when compared to other algorithms.

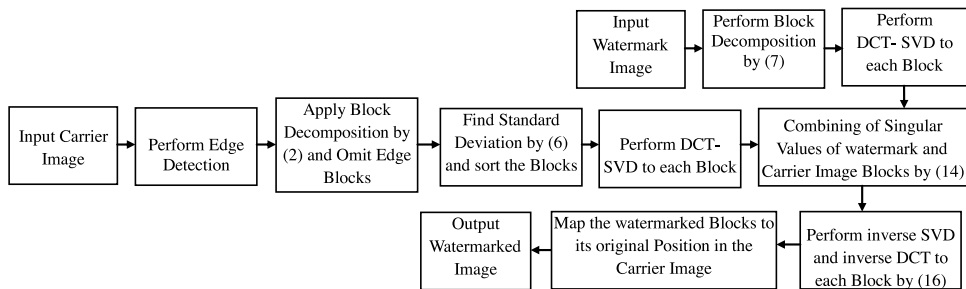


Fig. 1. Block Diagram of the proposed Watermark Embedding Scheme

The watermark extraction algorithm

The watermark extraction algorithm performs the inverse operation of the embedding process for analyzing the attached watermark for copyright process. Once the embedding process is over, the watermarked image, the block indices of both watermark and carrier images indicating where the embedding algorithm placed the extracted blocks. The U^w and V^w components of SVD are given as input to the extraction algorithm. The extraction algorithm is detailed through the following steps.

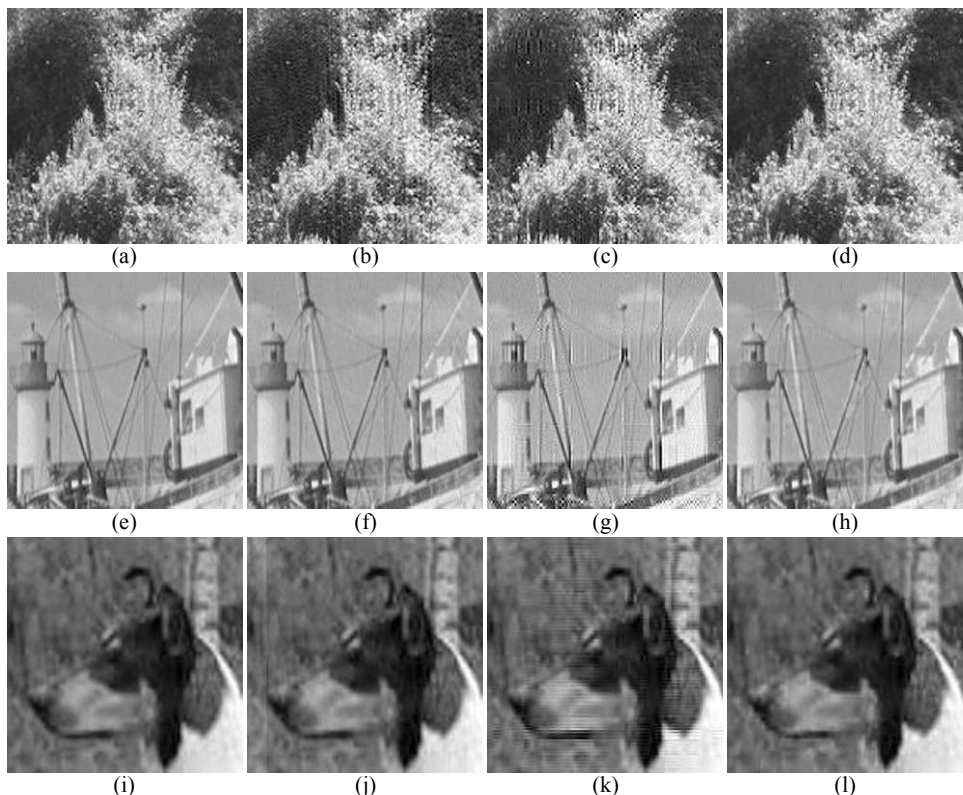


Fig. 2. Cropped watermarked images produced by Ray-Shine *et al.*, (2012) algorithm 1, Ray-Shine *et al.*, (2012) algorithm 2 and the proposed algorithms in the 2nd, 3rd and 4th column respectively against the different original crop images in the first column

Step 1: The extraction process starts by decomposing the blocks of input watermarked image A same as the watermark embedding algorithm by

$$\tilde{B}l_i = \{ A_{k,l} : i_l \leq k < i_l + n_l, j_l \leq l < j_l + n_l \} \quad (17)$$

where

$$\bigcup_{l=0}^{N-1} \tilde{B}l_i = \tilde{A} \quad (18)$$

and

$$(i_l, j_l) \in \left\{ (c_1 \cdot n_l, c_2 \cdot n_l) : 0 \leq c_1 < \frac{M_2}{4}, 0 \leq c_2 < \frac{N_2}{4} \right\} \quad (19)$$

Here (i_l, j_l) denotes the starting position of each non overlapping block

Step2: The algorithm determines the SVD of only the blocks $\tilde{B}l_i$ where the embedding algorithm attached the watermark blocks by looking the block indices ie., $i \in \text{Domain}(SBl)$ as

$$\tilde{U}_i \tilde{\Sigma}_i \tilde{V}_i = \tilde{B}l_i \quad (20)$$

$\text{Domain}(SBl)$ denotes the pixel positions of SBl .

Step 3: The $\tilde{\Sigma}_i^w$ component of the watermark image are extracted by separating carrier image components, $\tilde{\Sigma}_i^w$ by performing the inverse operation of Equation (14) as

$$\tilde{\Sigma}_i^w = \left(\tilde{\Sigma}_i - \Sigma_i^w \right) / \alpha \quad (21)$$

Step 4: The blocks $D\tilde{S}WBl_i$ of the watermark image, $SWBl$ are reconstructed according to the embedding order by performing inverse DCT as

$$D\tilde{S}WBl_i = IDCT \left(U_i^w \tilde{\Sigma}_i^w V_i^w \right) \quad (22)$$

Step 5: The individual $\tilde{S}WBl_i$ is mapped to the respective position by looking the mapping indices of watermark blocks to reconstruct the watermarked image, WBl .

The water mark extraction process first decomposed the watermarked image, \tilde{A} and selected the watermarked blocks by looking in to the block indices stored in *SBI*. These blocks are applied with forward DCT and SVD transformation to extract the attached watermark singular values, \sum_i^w . The watermarks singular values are extracted by using Equation (21) and the watermark blocks are reconstructed by performing the inverse DCT and SVD operations. Finally, the watermarked blocks are mapped to its respective positions to reconstruct the extracted watermarked image. Since the proposed algorithm has the advantages of DCT and SVD transforms in its watermarking and extraction processes, it has the ability to resist most of the external potential attacks. The proposed algorithm can provide better watermarked images and it stands as the major advantage of the proposed algorithm over other DCT-SVD based algorithms.

EXPERIMENTAL RESULTS

The proposed algorithm together with other prominent algorithms in the literature are tested over a wide variety of images of which Bridge (512×512), Boats (512×512), Dog (512×512), Lena (256×256), Cameraman (256×256), Rice (256×256) are used here for analyzing the subjective and objective performances. The Lena, Cameraman and Rice watermark images are respectively embedded in Bridge, Boats and Dog carrier images for experimental analysis. We used Alexander *et al.*, (2006), Emir *et al.*, (2004) and Ray-Shine *et al.*, (2012) algorithms for comparative analysis. The conceptual comparison of various algorithms used in the comparison analysis is made in Table 1. The peak signal-to noise ratio (PSNR), mean absolute error (MAE) and computation time (CT) in seconds are the metrics used for analyzing the objective performance of the watermarked images. We used Matlab 10 software in an Intel Core 2 Duo system of 2.6 GHz with 4MB RAM for testing the algorithms.

The PSNR is defined by

$$PSNR = 10 \log_{10} \left(\frac{(255)^2}{MSE} \right) \quad (dB) \quad (23)$$

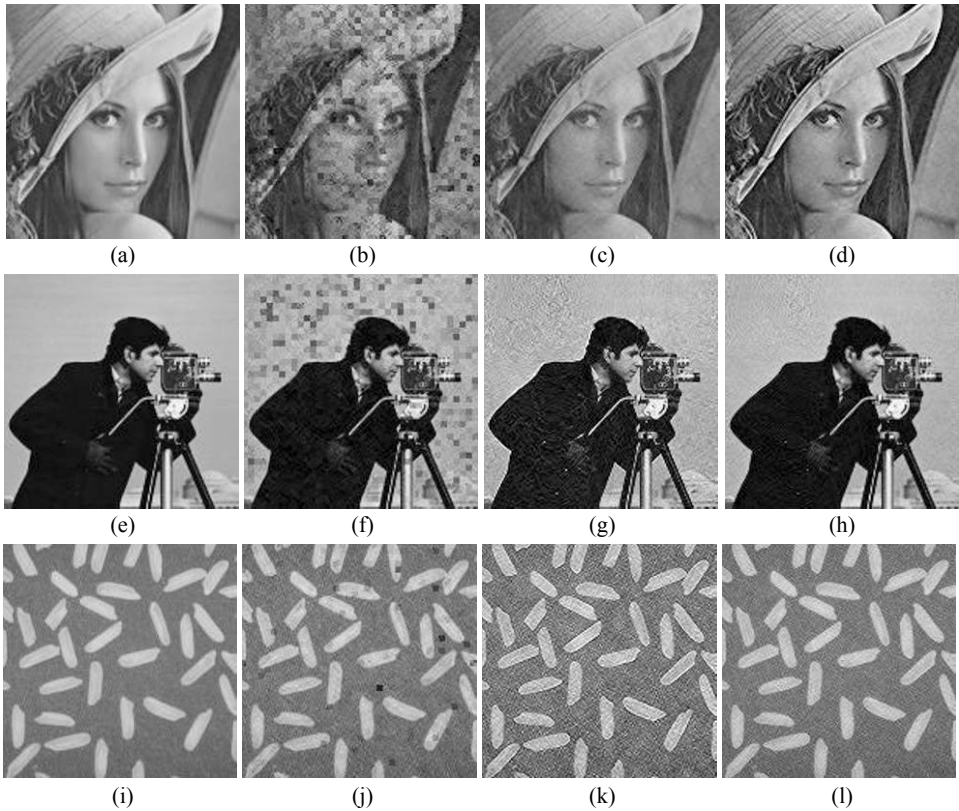


Fig. 3. Extracted cropped watermark images from Gaussian Noise (standard deviation: 0.001) attacked watermarked images by Alexander *et al.*, (2006), Emir *et al.*, (2004) and the proposed algorithms in the 2nd, 3rd and 4th column respectively against different original crop images in the first column

where the mean square error (MSE) of the watermarked image, \tilde{A} with the original carrier image, A of size $M_1 \times N_1$ is

$$MSE = \frac{1}{M_1 N_1} \sum_{i_1=0}^{M_1-1} \sum_{i_2=0}^{N_1-1} \left| \tilde{A}(i_1, i_2) - A(i_1, i_2) \right|^2 \quad (24)$$

The mean absolute error (MAE) of the watermarked image, \tilde{A} from original image, A is given by

$$MAE = \frac{1}{M_1 N_1} \sum_{i_1=0}^{M_1-1} \sum_{i_2=0}^{N_1-1} \left| \tilde{A}(i_1, i_2) - A(i_1, i_2) \right| \quad (25)$$

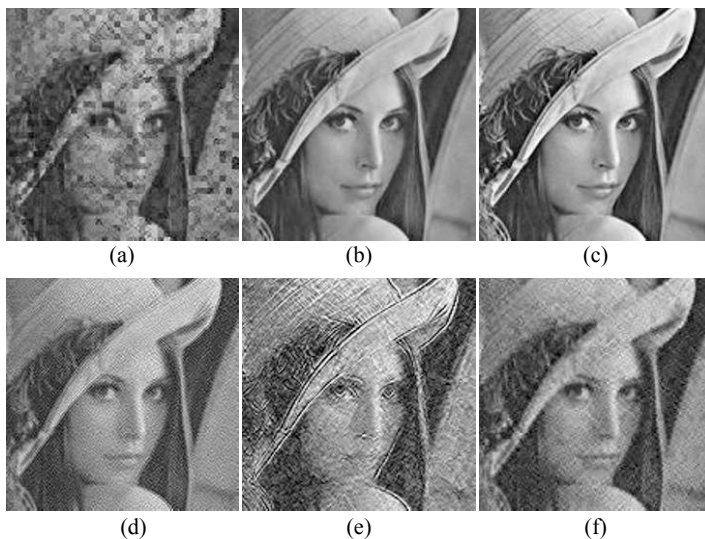


Fig. 4. Cropped Lena watermark images extracted from Histogram Equalization and Guassian filtering (5×5) attacked Bridge watermarked images respectively in each row by Alexander *et al.*, (2006), Emir *et al.*, (2004) and the proposed algorithms in the 1st, 2nd and 3rd column respectively

The PSNR, MAE and computation time (CT) values experimentally obtained by Alexander *et al.*, (2006), Emir *et al.*, (2004) and Ray-Shine *et al.*, (2012) algorithm 1, Ray-Shine *et al.*, (2012) algorithm 2 and the proposed algorithms are shown in Table 2. Note that the objective and subjective comparisons are made with the algorithms that attach similar sized watermarks. The strength of watermarking α is set to 0.1 for all algorithms to uniformly evaluate PSNR and MAE of watermarked images. For Alexander *et al.*, (2006), Emir *et al.*, (2004) and Ray-Shine *et al.*, (2012) algorithms, watermarks are attached to only one subband / block which provides higher PSNR to ensure that the watermark contents attached are equal for all algorithms.

Table 1. Conceptual comparative analysis of different algorithms

Notes	Alexander <i>et al.</i> , (2006)	Emir <i>et al.</i> , (2004)	Ray-Shine <i>et al.</i> , (2012) algorithm 1	Ray-Shine <i>et al.</i> , (2012) algorithm 2	Proposed Algorithm
Transforms	DCT-SVD	DWT-SVD	DCT-SVD	DWT-SVD	DCT-SVD
Subband Embedding	All	All	Two	Two	one
Watermark Transform	DCT-SVD	SVD	SVD	SVD	DCT- SVD
Carrier Image Size	512 × 512	512 × 512	512 × 512	512 × 512	512 × 512
Watermark Size	256 × 256	256 × 256	256 × 256	256 × 256	256 × 256
Type of Watermark	Gray	Gray	Gray	Gray	Gray

Pearson's correlation coefficient (PCC) is the objective metric used for analyzing the quality of extracted watermarks in cases where the potential attacks occur during transmission of watermarked images. Pearson's correlation provides the degree of linear relationship between carrier vector of singular values, Σ^w and extracted vector of singular values, $\tilde{\Sigma}^w$ and is mathematically given by

$$PCC = \frac{\sum (\Sigma^w - \overline{\Sigma^w}) \left(\tilde{\Sigma}^w - \overline{\tilde{\Sigma}^w} \right)}{\sqrt{\sum (\Sigma^w - \overline{\Sigma^w})^2} \sqrt{\sum \left(\tilde{\Sigma}^w - \overline{\tilde{\Sigma}^w} \right)^2}} \quad (26)$$

The notations $\overline{\Sigma^w}$ and $\overline{\tilde{\Sigma}^w}$ used here are the mean of vector of singular values, Σ and the mean of extracted vector of singular values, $\tilde{\Sigma}^w$. From Table 2, it is very clear that the proposed algorithm provides better MAE and PSNR values when compared to other algorithms. The watermarked image outputs produced by Ray-Shine *et al.*, (2012) algorithm 1, Ray-Shine *et al.*, (2012) algorithm 2 and the proposed algorithm for visual analysis are provided in Figure 2. The outputs produced by proposed algorithm provide better quality watermarked images than other algorithms.

Table 2. MAE and PSNR of watermarked images produced by different algorithms

Algorithms	Criteria	Images		
		Lena in Bridge	Cameraman in Boats	Rice in Dog
Alexander <i>et al.</i> , (2006)	MAE	7.8881	7.8427	6.7793
	PSNR	25.6975	25.5824	26.6136
	CT	2.7242	2.7251	2.7371
Emir <i>et al.</i> , (2004)	MAE	8.9540	8.9452	7.7683
	PSNR	25.6975	25.5824	26.6136
	CT	2.7861	2.7914	2.7872
Ray-Shine <i>et al.</i> , (2012) algorithm 1	MAE	5.4780	5.3086	4.6698
	PSNR	29.2877	29.1727	30.2038
	CT	2.5375	2.5264	2.5393
Ray-Shine <i>et al.</i> , (2012) algorithm 2	MAE	6.9141	7.1363	6.4993
	PSNR	29.2877	29.1727	29.8212
	CT	2.5462	2.5473	2.5452
Proposed Algorithm	MAE	2.4262	2.4665	1.9301
	PSNR	32.6874	31.9044	33.6342
	CT	2.7341	2.7358	2.7337

The watermarked outputs produced by the proposed algorithm provide better objective metrics with high perception quality because it attaches the watermark contents to only the selected less sensitive areas of the carrier image. For testing the resistive power of different algorithms against external potential attacks we used Gaussian noise, Gaussian filtering, histogram equalization, JPEG compression, rescaling, image unsharpening, gamma correction, salt & pepper impulse noise, pixelate and rotation based potential attacks. The watermark images extracted from different watermarked images affected with Gaussian noise by Alexander *et al.*, (2006), Emir *et al.*, (2004) and the proposed algorithm are shown in Figure 3. The extracted Lena watermark images from watermarked Bridge image affected with histogram equalization and Gaussian filtering by Alexander *et al.*, (2006), Emir *et al.*, (2004) and the proposed algorithms are provided in Figure 4. For Alexander *et al.*, (2006) and Emir *et al.*, (2004) algorithms, we selected the best visual watermark extracted from all subbands / blocks.

Table 3. PCC Values Obtained for Lena Watermark Image Extracted from Watermarked Bridge Image Affected with Various Potential Attacks by different Algorithms

Algorithms	Ray-Shine <i>et al.</i> , (2012) algorithm 1	Ray-Shine <i>et al.</i> , (2012) algorithm 2	Emir <i>et al.</i> , (2004)	Alexander <i>et al.</i> , (2006)	Proposed Algorithm
PSNR of Watermarked Image	29.421	29.562	29.814	29.567	29.945
Potential Attacks					
Gaussian Noise 0.001	0.854	0.854	0.996	0.995	0.980
Gaussian Filtering 3*3	0.946	0.942	0.970	0.984	0.995
Gaussian Filtering 5*5	0.946	0.941	0.970	0.983	0.995
Gaussian Filtering 7*7	0.946	0.941	0.970	0.983	0.995
Histogram Equalization	0.673	0.804	0.934	0.952	0.975
Jpeg Compression 75% Quality	0.191	0.227	0.867	0.395	0.950
Jpeg Compression 50% Quality	0.184	0.218	0.869	0.461	0.950
Rescaling 512->256->512	0.726	0.812	0.917	0.941	0.979
Rescaling 512->1024->512	0.969	0.980	0.996	0.996	0.997
Image Unsharpening	0.440	0.583	0.790	0.852	0.912
Gamma Correction 0.8	0.978	0.987	0.998	1.000	0.974
Gamma Correction 0.6	0.909	0.938	0.981	1.000	0.956
Salt & Pepper Impulse Noise 1%	0.685	0.683	0.976	0.965	0.972
Salt & Pepper Impulse Noise 5%	0.384	0.378	0.721	0.730	0.924
Pixelate 2*2	0.703	1.000	1.000	0.968	0.987
Pixelate 4*4	0.464	0.422	0.661	0.875	0.964
Rotate 20 ⁰	0.174	0.132	-0.353	0.473	0.659

It is very clear that the extracted watermark images produced by the proposed algorithm are better in majority of cases when compared to other algorithms. For the proposed algorithm, we calculated PCC values after reconstructing the full singular value image from all the extracted and attached watermark blocks to make efficient comparison with other algorithms. The higher positive and lower negative values in the range $[-1, +1]$ of PCC values show high similarity and larger deviation among embedded and extracted watermark images respectively. In order to measure PCC of extracted watermark images in the case of potential attack deviated image, we fixed the PSNR of the watermarked image around 30db by varying the strength parameter, α .

Table 4. PCC values obtained for cameraman watermark image extracted from watermarked boats image affected with various potential attacks by different algorithms

Algorithms	Ray-Shine <i>et al.</i> , (2012) algorithm 1	Ray-Shine <i>et al.</i> , (2012) algorithm 2	Emir <i>et al.</i> , (2004)	Alexander <i>et al.</i> , (2006)	Proposed Algorithm
PSNR of Watermarked Image	29.471	29.572	29.921	29.878	29.895
Potential Attacks					
Gaussian Noise 0.001	0.856	0.857	0.992	0.992	0.989
Gaussian Filtering 3*3	0.949	0.965	0.987	0.992	0.998
Gaussian Filtering 5*5	0.948	0.965	0.987	0.992	0.998
Gaussian Filtering 7*7	0.948	0.965	0.987	0.992	0.998
Histogram Equalization	0.747	0.619	0.819	0.922	0.945
Jpeg Compression 75% Quality	0.292	0.238	0.817	0.470	0.930
Jpeg Compression 50% Quality	0.289	0.250	0.820	0.572	0.929
Rescaling 512->256->512	0.715	0.888	0.966	0.965	0.990
Rescaling 512->1024->512	0.965	0.990	0.999	0.998	0.999
Image Unsharpening	0.790	0.861	0.938	0.954	0.944
Gamma Correction 0.8	0.986	0.986	0.998	1.000	0.982
Gamma Correction 0.6	0.928	0.936	0.985	0.999	0.961
Salt & Pepper Impulse Noise 1%	0.709	0.697	0.957	0.963	0.980
Salt & Pepper Impulse Noise 5%	0.396	0.403	0.654	0.694	0.932
Pixelate 2*2	0.691	1.000	1.000	0.974	0.994
Pixelate 4*4	0.469	0.493	0.787	0.911	0.982
Rotate 20°	0.182	0.148	-0.391	0.495	0.741

The PCC values of Lena, Cameraman and Rice watermark images respectively extracted from watermarked Bridge, Boats and Dog images affected with various potential attacks by Alexander *et al.*, (2006), Emir *et al.*, (2004) and Ray-Shine *et al.*, (2012) algorithm 1, Ray-Shine *et al.*, (2012) algorithm 2 and the proposed algorithm

are tabulated in Table 3, Table 4 and Table 5. From the obtained PCC values, it is very clear that the proposed algorithm is capable of producing better objective values in majority of cases than that of other competitive algorithms.

Table 5. PCC Values Obtained for Rice Watermark Image Extracted from Watermarked Dog Image Affected with Various Potential Attacks by different Algorithms

Algorithms	Ray-Shine <i>et al.</i> , (2012) algorithm 1	Ray-Shine <i>et al.</i> , (2012) algorithm 2	Emir <i>et al.</i> , (2004)	Alexander <i>et al.</i> , (2006)	Proposed Algorithm
PSNR of Watermarked Image	29.512	29.578	29.891	29.902	29.965
Potential Attacks					
Gaussian Noise 0.001	0.828	0.827	0.974	0.984	0.995
Gaussian Filtering 3*3	0.978	0.984	0.998	0.999	0.999
Gaussian Filtering 5*5	0.978	0.983	0.998	0.999	0.999
Gaussian Filtering 7*7	0.978	0.983	0.998	0.999	0.999
Histogram Equalization	0.921	0.901	0.959	0.979	0.976
Jpeg Compression 75% Quality	0.227	0.254	0.886	0.469	0.955
Jpeg Compression 50% Quality	0.227	0.260	0.886	0.469	0.955
Rescaling 512->256->512	0.869	0.950	0.990	0.988	0.995
Rescaling 512->1024->512	0.991	0.996	1.000	1.000	1.000
Image Unsharpening	0.948	0.991	0.998	0.999	0.971
Gamma Correction 0.8	0.996	0.996	1.000	1.000	0.991
Gamma Correction 0.6	0.981	0.978	1.000	0.999	0.978
Salt & Pepper Impulse Noise 1%	0.634	0.635	0.919	0.925	0.985
Salt & Pepper Impulse Noise 5%	0.330	0.281	0.675	0.631	0.937
Pixelate 2*2	0.792	1.000	1.000	0.988	0.998
Pixelate 4*4	0.514	0.547	0.864	0.938	0.989
Rotate 20°	0.197	0.154	-0.379	0.501	0.727

It is to be noted that DWT has advantages over DCT in providing good localization of images in both time and spatial domain and will provide good resistance towards Gamma correction, Pixelate and geometrical scaling while DCT provides better resistance for the watermarked images in case of compression, noise and filtering and contrast enhancement based potential attacks (Jie *et al.*, 2006; Koch *et al.*, 1996; Zhou *et al.*, 2004). Unlike the other algorithms, since we attached watermark blocks to the selected blocks, the proposed algorithm always have good PSNR values even though the strength parameter, α is high. This enables the proposed algorithm to produce better PCC values for most of the cases. For experimental purposes we set the threshold, T to be 75 to find sharp edges.

CONCLUSION

An effective watermarking scheme by incorporating singular vector decomposition, discrete cosine transform and homogeneity information is proposed. The algorithm avoids the decomposed carrier image blocks that contain sharp edges, when attaching watermark blocks, since watermark embedding in these blocks produces much distortion in the watermarked images. Experimental results showed that the proposed algorithm is capable of producing good quality watermarked images and are least sensitive to potential attacks than the other algorithms used in the comparative study.

REFERENCES

- Alexander, S., Scott, D. & Ahmet, M. E. 2006.** Secure DCT-SVD Domain Image Watermarking: Embedding Data in All Frequencies. Proceedings of the Image Processing seminar. Brooklyn College, New York, USA.
- Bhosale, S., Thube, G., Jangam, P. & Borse, R. 2012.** Employing SVD and Wavelets for Digital Image Forensics and Tampering Detection. Proceedings of the IEEE International Conference on Advances in Mobile Network. Communication and its Applications. Bangalore, India.
- Chen, Y., Weiyu, Y. & JiuChao, F. 2012.** A digital watermarking based on discrete fractional fourier transformation DWT and SVD. Proceedings of the IEEE International Conference on Control and Decision. Taiyuan, China.
- Chih-Chin, L. 2010.** Digital Image Watermarking Using Discrete Wavelet Transform and Singular Value Decomposition. IEEE Transactions on Instrumentation and Measurement, **59**(11): 3060–3063.
- Coatrieux, G., Wei, P., Cuppens-Boulahia, N., Cuppens, F. & Roux, C. 2012.** Reversible Watermarking Based on Invariant Image Classification and Dynamic Histogram Shifting. IEEE Transactions on Information forensics and security, **8**(1):111-120.
- Emir, G. & Ahmet, M. E. 2004.** Robust DWT SVD domain image watermarking: embedding data in all frequencies. Proceedings of the International Multimedia Conference. Magdeburg, Germany.
- Gonzalez, R. C. & Richard E. W. 2008.** Digital image processing. Prentice Hall, New Jersey, USA.
- Hailiang, S., Nan, W., Zihui, W., Yue, W., Huiping, Z. & Yanmin, Y. 2012.** RST invariant image watermarking scheme using DWT-SVD. Proceedings of the IEEE International Symposium on Instrumentation & Measurement, Sensor Network and Automation. Sanya, China.
- Ingemar, J. C., Matthew, L. M., Jeffrey, A. B., Jessica, F. & Ton, K. 2008.** Digital Watermarking and Steganography. Morgan Kaufmann Publishers, Elsevier, Burlington, USA.
- Ishikawa, Y., Kazutake, U. & Kazuhisa, Y. 2012.** Optimization of Size of Pixel Blocks for Orthogonal Transform in Optical Watermarking Technique. Journal of Display Technology, **8**(9): 505-510.
- Jen-Sheng, T., Win-bin, H. & Yau-Hwang, K. 2011.** On the Selection of optimal Feature Region Set for Robust Digital Image Watermarking. IEEE Transactions on Image Processing, **20**(3): 735–743.
- Jie, L., Xiamu N. & Wenhai K. 2006.** Image Watermarking based on Singular Value Decomposition. Proceedings of the International Conference on Intelligent Information Hiding and Multimedia Signal Processing. California, USA.
- Juergen, S. 2005.** Digital Watermarking for Digital Media. Information Science Publishing, Hershey, USA.
- Kandpal, H., Hitanshu, K. & Manoj, K. 2012.** Wave atom-SVD based digital image watermarking

- scheme. Proceedings of the IEEE Students Conference on Engineering and Systems. Allahabad, Uttar Pradesh, India.
- Koch E., Rindfrey J. & Zhao J. 1994.** Copyright protection for multimedia data. Proceedings of the Digital media and electronic publishing, USA.
- Mason, A. J., Salmon, R. A., Werner, O. H. & Devlin, J. E. 2000.** User requirements for watermarking in broadcast applications. Proceedings of the International Broadcasting Convention. Amsterdam, Netherlands.
- Mitra, P., Gunjan, R. & Gaur, M. S. 2012.** A multi-resolution watermarking based on contour let transform using SVD and QR decomposition. Proceedings of the IEEE International Conference on Recent Advances in Computing and Software Systems. Chennai, India.
- Paul, P. B. & Ma, X. 2005.** Image Adaptive Watermarking Using Wavelet Domain Singular Value Decomposition. IEEE Transactions on Circuits and Systems for Video Technology, **15**(1): 96-102.
- Ray-Shinc, R., Shi-Jinn, H., Jui-Lin, L., Tzong-Wang, K. & Rong-Jian, C. 2012.** An improved SVD-based watermarking technique for copyright protection. Journal Expert Systems with Applications, **39**(1): 673-689.
- Vargas, L. & Elizabeth, V. 2013.** An Implementation of Reversible Watermarking for Still Images. Latin America IEEE Transactions (Revista IEEE America Latina), **11**(1): 54-59.
- Varghese, J., Hussain, O. B., Babu, B., Basheer, J. M., Subash, S., Saadi, M. R. & Khan, M. S. 2014.** An efficient DCT-SVD based algorithm for digital image watermarking. Proceedings of the IEEE International Carnahan Conference on Security Technology. Rome, Italy.
- Walia, E. & Anu, S. 2013.** Fragile and blind watermarking technique based on Weber's law for medical image authentication. IET Computer Vision, **7**(1): 9-19.
- Wang, W., Aidong, M. ., Bo, Y. & Xiaobo, C. 2011.** A novel robust zero watermarking scheme based on DWT and SVD. Proceedings of the IEEE International Conference on Image and Signal Processing. Shanghai, China.
- Wang, C., Jiangqun, N. & Jiwu, H. 2012.** An Informed Watermarking Scheme Using Hidden Markov Model in the Wavelet Domain. IEEE Transactions on Information Forensics and Security, **7**(3) :853-867.
- Wu, Y. 2005.** On the security of an SVD-based ownership watermarking. IEEE Transactions on Multimedia, **7**(4): 624-627.
- Yang, C. H. & Tsai, M. H. 2010.** Improving histogram-based reversible data hiding by interleaving predictions. IET Image processing, **4**(4):223-234.
- Zareian, M. & Hamid, R. T. 2013.** Robust quantization index modulation-based approach for image watermarking. IET Image Processing, **7**(5): 432-441.
- Zhou B. & Chen. A. 2004.** Geometric Distortion Resilient Image Watermarking Algorithm Based on SVD. Chinese Journal of Image and Graphics, **9**(4): 506-512.

Open Access: This article is distributed under the terms of the Creative Commons Attribution License (CC-BY 4.0) which permits any use, distribution, and reproduction in any medium, provided the original author(s) and the source are credited.

Submitted: 07-06-2014

Revised: 12-10-2014

Accepted: 20-10-2014